The Journal of Comparative Neurology 517:177–192 (2009)
Research in Systems Neuroscience

Transmitter-Phenotypes of Commissural Interneurons in the Lumbar Spinal Cord of Newborn Mice

CARLOS ERNESTO RESTREPO,[1] LINE LUNDFALD,[1] GABOR SZABÓ,[2] FERENC ERDÉLYI,[2] HANNS ULRICH ZEILHOFER,[3] JOEL C. GLOVER,[4] AND OLE KIEHN[1]*

[1]Mammalian Locomotor Laboratory, Department of Neuroscience, Karolinska Institutet, 17177 Stockholm, Sweden
[2]Gene Technology and Developmental Neuroscience, Institute of Experimental Medicine, H-1450, Budapest, Hungary
[3]Institute of Pharmacology and Toxicology, University of Zurich, Zurich, Switzerland
[4]Department of Physiology, University of Oslo, 0317 Oslo, Norway

ABSTRACT

Commissural interneurons (CINs) are a necessary component of central pattern generators (CPGs) for locomotion because they mediate the coordination of left and right muscle activity. The projection patterns and relative locations of different classes of CINs in the ventromedial part of the rodent lumbar cord have been described (Eide et al. [1999] J Comp Neurol 403:332–345; Stokke et al. [2002] J Comp Neurol 446:349–359; Nissen et al. [2005] J Comp Neurol 483:30–47). However, the distribution and relative prevalence of different CIN neurotransmitter phenotypes in the ventral region of the mammalian spinal cord where the locomotor CPG is localized is unknown. In this study we describe the relative proportions and anatomical locations of putative inhibitory and excitatory CINs in the lumbar spinal cord of newborn mice. To directly visualize potential neurotransmitter phenotypes we combined retrograde labeling of CINs with in situ hybridization against the glycine transporter, GlyT2, or the vesicular glutamate transporter, vGluT2, in wildtype mice and in transgenic mice expressing eGFP driven by the promoters of glutamic acid decarboxylase (GAD) 65, GAD67, or GlyT2. Our study shows that putative glycinergic, GABAergic, and glutamatergic CINs are expressed in almost equal numbers, with a small proportion of CINs coexpressing GlyT2 and GAD67::eGFP, indicating a putative combined glycinergic/GABAergic phenotype. These different CIN phenotypes were intermingled in laminas VII and VIII. Our results suggest that glycinergic, GABAergic, and glutamatergic CINs are the principal CIN phenotypes in the CPG region of the lumbar spinal cord in the newborn mouse. We compare these results to descriptions of CIN neurotransmitter phenotypes in other vertebrate species. J. Comp. Neurol. 517:177–192, 2009.

Indexing terms: locomotion; CPG; commissural interneurons; spinal cord; motor neurons; glutamate; GABA; glycine

The timing and coordination of rhythmic movements such as swimming and walking in vertebrates are in large part produced by neural networks localized in the spinal cord. These networks are called central pattern generators (CPGs) because they can generate functional rhythmic motor activity independently of sensory input. A critical function of CPGs is to coordinate muscular activity on the left and right sides of the body. This CPG function is mediated by activity in commissural interneurons (CINs), whose axons cross the midline to synapse on neurons on the opposite side. Initial studies of the functional organization of CINs in vertebrate CPGs were carried out in aquatic vertebrates (Buchanan, 1982, 1999; Buchanan and Cohen, 1982; Clarke and Roberts, 1984; Dale, 1985; Buchanan and Grillner, 1987; Fetcho, 1990; Soffe et al., 2001; Grillner, 2003). These studies unveiled inhibitory glycinergic descending CINs (dCINs) as the CPG neurons mediating left–right alternation during swimming. The dCINs serve this role by projecting to and inhibiting contralateral motor neurons and contralateral CPG interneurons. Glutamatergic CINs have also been identified in the lamprey and zebrafish (Higashijima et al., 2004a,b; Biro et al., 2008). In the zebrafish these crossed excitatory CINs are also thought to play a role

Additional Supporting Information may be found in the online version of this article.

Grant sponsor: National Institutes of Health (NIH); Grant number: 5R01NS40795-09 (to O.K.); Grant sponsor: Swedish Research Council (to O.K.); Grant sponsor: Wings for Life (to O.K.); Grant sponsor: Hedlund Foundation (to O.K.); Grant sponsor: Söderberg Foundation (to O.K.); Grant sponsor: the HFSP (to J.C.G., O.K.); Grant sponsor: Norwegian Research Council (to J.C.G.).

*Correspondence to: Professor Ole Kiehn, Department of Neuroscience, Karolinska Instiutet, Retzius väg 8, 17177 Stockholm, Sweden.
E-mail: O.Kiehn@ki.se

Received 16 January 2009; Revised 20 March 2009; Accepted 4 July 2009

DOI 10.1002/cne.22144

Published online July 16, 2009 in Wiley InterScience (www.interscience.wiley.com).

in mediating slow swimming (McLean et al., 2007). Studies of locomotor-related CIN projections in mammals have described the presence of both direct excitatory and direct inhibitory CIN connections to contralateral motor neurons (Butt and Kiehn, 2003; Jankowska et al., 2003, 2005a,b, 2006; Quinlan and Kiehn, 2007) as well as polysynaptic inhibitory and excitatory CIN pathways onto motor neurons (Butt and Kiehn, 2003; Jankowska et al., 2005b, 2006; Nishimaru et al., 2006; Quinlan and Kiehn, 2007). The synaptic nature of these CIN connections has been shown electrophysiologically in rats and mice to be either glutamatergic, glycinergic, or combined glycinergic/GABAergic, whereas the polysynaptic inhibitory connections have been shown to be mediated by glutamatergic CINs synapsing onto combined glycinergic/GABAergic interneurons (Butt and Kiehn, 2003; Quinlan and Kiehn, 2007). Likewise, anatomical studies in the cat and rat have shown that CIN axon terminals in close proximity to motor neurons as well as in the intermediate area of the ventral spinal cord are putatively glutamatergic, glycinergic, or GABAergic (Bannatyne et al., 2003; Weber et al., 2007). This complex system of CINs appears to be involved in segmental left–right alternation and in segmental and intersegmental crossed motor synergies during locomotion in tetrapods (Kiehn, 2006). No description has yet been made, however, of the distribution and relative prevalence of different CIN neurotransmitter phenotypes of the entire population of CINs in the ventral spinal cord (the intermediate area and lamina VIII) where the locomotor CPG is localized (Kiehn and Kjaerulff, 1998).

Here we visualize putative CIN neurotransmitter phenotypes by combining retrograde labeling of the entire CIN population in lumbar segments of the ventral spinal cord of newborn mice with in situ hybridization and neurotransmitter-specific GFP expression in transgenic mice. Our results show that putative glycinergic, GABAergic, and glutamatergic CINs are expressed in almost equal numbers, with a small proportion of CINs potentially having a combined glycinergic/GABAergic phenotype. These different CIN phenotypes were found in overlapping regions within the ventral spinal cord, with putative GABAergic CINs occupying a somewhat more medial position. We thus provide anatomical information that is essential to understand the complex functions of CINs in the mouse spinal cord and which allows a comparison with the organization of CINs in other vertebrate CPGs.

MATERIALS AND METHODS

Animals

All experimental procedures were approved by the Swedish Animal Welfare Agency. Wildtype mice (C57BL/6) were used to assess potential glutamatergic and glycinergic phenotypes of CINs using immunohistochemistry or in situ hybridization against mRNA. Putative glycinergic CINs were also visualized in GlyT2::eGFP mice that express eGFP under the control of the promoter for the neuronal glycine transporter 2 gene (*GlyT2*) (Zeilhofer et al., 2005). eGFP was placed in frame at the beginning of exon 2 in the Glyt2 gene in a 179,508 bp-long BAC-clone that contained the entire GlyT2 gene and additional 105 kb and 21 kb of DNA flanking the gene upstream and downstream, respectively (Zeilhofer et al., 2005). Putative GABAergic CINs were visualized in glutamic acid decarboxylase (GAD) 67::eGFP knockin mice (Tamamaki et al., 2003) and/or in transgenic mice expressing eGFP under the control of the GAD65 promoter. In the GAD67::eGFP knockin mouse, cDNA encoding eGFP was targeted to exon 1 encoding GAD67. The transgene in the GAD65 mouse includes a 6.3-kb segment of the GAD65 gene covering the first two exons, the intron in between, and a 5.5-kb upstream region of the gene. eGFP without its own translation site was fused in-frame with exon 2 (Lopez-Bendito et al., 2004; Hughes et al., 2005).

The present study shows that eGFP reliably labels putative glycinergic neurons in the spinal cord of the Glyt2::eGFP mouse (see Results). The eGFP expression in the GAD67::eGFP mouse has previously been thoroughly described and verified in brain (Tamamaki et al., 2003) and spinal cord tissue (Huang et al., 2008a,b). These studies showed using double immunohistochemistry or combined methods of immunohistochemistry and in situ hybridization that the vast majority (80–96%) of GFP-positive neurons in the GAD67::eGFP mouse are either GAD67 mRNA-positive or GABA-immunoreactive. None of these studies reported ectopic expression. Furthermore, in a previous study known groups of excitatory interneurons in the spinal cord were not GFP-positive in the GAD67::eGFP mouse (Lundfald et al., 2007). The GAD65::eGFP transgenic mouse line has been shown to label many GAD65-positive terminals in the gray matter of the spinal cord, although some synaptic terminals express GAD65 immunoreactivity without GFP expression (Hughes et al., 2005). Moreover, the distribution of the GAD65-GFP in the spinal cord was observed to be identical to that seen in nontransgenic animals with some apparent ectopic expression in fibers in the dorsal column white matter.

Dissection

Spinal cords were prepared from wildtype and heterozygous eGFP-expressing mice aged 0–2 days (P0–P2, where P0 is day of birth). The animals were decapitated under deep isoflurane anesthesia after which they were eviscerated as described previously (Kiehn and Kjaerulff, 1996). The thoracolumbar spinal cord (Th11-L6) was then surgically isolated and transferred to a Petri dish filled with low Ca^{2+} Ringer's solution (in mM: 111.14 NaCl, 3.09 KCl, 25 $NaHCO_3$, 1.10 KH_2PO_4, 3.73 $MgSO_4$, 0.25 $CaCl_2$, and 11.10 glucose aerated with 5% CO_2 in O_2 to maintain pH at 7.4).

Dextran labeling and fixation

After dissection, CINs were retrogradely labeled by applying crystals of a fluorescent dextran amine tracer, Texas Red dextran amine (TxRDA, 3,000 kDa) in the ventral commissure of the L2 segment as previously described (Glover, 1995; Stokke et al., 2002; Nissen et al., 2005) (Fig. 1). Spinal cords that were accidentally labeled dorsal to the central canal were excluded from further analysis.

Preparations were then incubated for 5–7 hours in the dark in oxygenated normal Ringer's solution (with normal calcium and magnesium concentrations: 2.5 mM $CaCl_2$ and 1.43 $MgSO_4$) at room temperature.

After incubation the spinal cords were immersed in 4% paraformaldehyde (PFA) in phosphate-buffered saline (PBS) overnight at 4°C. The fixed tissue was then cryoprotected by incubation in 20% sucrose in PBS overnight at 4°C. Twelve μm cryosections were mounted on Menzer-glaser SuperFrost slides. The slides were kept at −80°C until used for immunohistochemistry or in situ hybridization.

Immunohistochemistry

Slides bearing sections for immunohistochemistry were washed with PBS and incubated with 5% donkey serum (Jackson Immunochemicals, West Grove, PA) for 1 hour in PBS to block nonspecific binding sites. Then the slides were placed in PBS containing rat antiglycine antibody (Table 1) or rabbit anti-GFP (Table 1) overnight at 4°C.

After washing with PBS the slides were incubated with Carbocyanine dye (Cy2 or Cy3)-conjugated donkey antirat or antirabbit antibody (1:500) diluted in blocking solution at 4°C overnight. The slides were then washed with PBS. Lastly, to confirm the colocalization of retrograde labeling (TxRDA) with immunostaining, cell nuclei were stained by incubating slides with Hoechst 33258 (2′-(4-hydroxyphenyl)-5-(4-methyl-1-piperazinyl)-2,5′-bi(1H-benzimidazole) or To-Pro-3 (monomeric cyanine nucleic acid stain) (1:10,000) for 5 minutes at room temperature (Bink et al., 2001; Lundfald et al., 2007). Excess Hoechst/To-Pro-3 was removed by washing with PBS (pH 7.4). Slides were coverslipped with 50% glycerol in PBS.

Antibody specificity

Optimal antibody concentrations were determined by increasing the concentration from that which gave negligible signal to that which gave a reliable visualization of cell bodies. No signal was observed in control sections when the primary antibody was omitted. The glycine antibody was made by conjugating glycine to porcine thyroglobulin by using PFA. It was developed by David Pow (University of Brisbane, Brisbane), has been extensively tested for specificity to glycine relative to other amino acids including GABA and glutamate as well as the carrier protein (Pow et al., 1995; and pers. commun.), and has been used in retina (Pow et al., 1995) and spinal cord (Allain et al., 2006). The staining pattern of the glycine antibody exhibited cellular morphology and a distribution in the mouse spinal cord that was identical to those previously reported in the rat (Allain et al., 2006). Staining was also eliminated by preincubation with the diluted antiserum (1:7,000) with three different dilutions (100%, 10%, and 0.1%) of a glycine-PFA-porcine-thyroglobolin conjugate (prepared as in Pow et al., 1995). Similar to previous reports (Allain et al., 2006), preabsorbtion with dilutions (100%, 10%, and 0.1%) of a glycine (3.75 mg/mL)-PFA-bovine serum albumin (BSA) (5 mg/mL) conjugate also diminished and eventually eliminated the staining. We also did preabsorbtion with porcine thyroglobulin in the spinal cord and did not see diminished glycine immunoreactivity (see also Allain et al., 2006). The staining pattern of the GFP antibody also exhibited cellular morphology and a distribution in the mouse spinal cord that was identical to those previously reported (e.g., Tamamaki et al., 2003). Furthermore, we evaluated the specificity of the GFP antibody in sections from eGFP-positive mice using the native eGFP fluorescence as control and a Cy3-conjugated antirabbit antibody to visualize the GFP antibody binding. This test showed colocalization between the native eGFP fluorescence and the GFP antibody staining and no ectopic staining (data not shown). Moreover, the GFP antibody did not label cells in sections from wildtype mice.

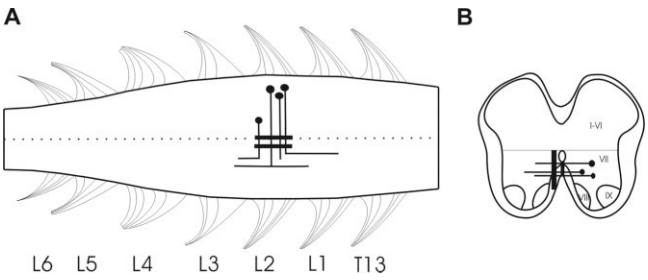

Figure 1.
Schematic drawing of the retrograde labeling procedure. The drawing depicts the two methodological approaches used in this study: retrograde labeling of CINs by application of TxRDA at a parasagittal or a midline cut. In both cases the cut was made ventral to the central canal and along the entire length of the second lumbar segment, L2. TxRDA application indicated by the thick lines, CIN axons by the thin lines. **A:** View of the spinal cord from the ventral surface. **B:** Transverse section.

In situ hybridization

Putative glutamatergic and glycinergic neurons were visualized using digoxygenin (DIG)-based in situ hybridization against mRNA encoding either a vesicular transporter (glutamate) or a cell membrane transporter (glycine). For glutamate we used a probe for vesicular glutamate transporter 2 (vGluT2) mRNA similar to the one we have used previously (probe for bp 1–811 of vGluT2-cDNA, gift from Dr. M. Goulding, Salk Institute) (Lundfald et al., 2007). To visualize glycinergic neurons we used a probe for neuronal glycine transporter 2 (GlyT2) transcribed from a 3.1-kb partial GlyT2-cDNA (gift from Dr. Nelson, Tel Aviv) (Liu et al., 1993). This probe is for nearly the full length of the coding sequence of the GlyT2 gene (probe for 1–3.508 bp) and has previously been shown to reliably label putative glycinergic cells in the rat brainstem (Stornetta et al., 2004). The GlyT2 sequence used for creating the probe came from a rat cDNA library. However, BLAST alignment showed 95% similarity between the rat and the mouse GlyT2 sequence. Moreover, we specifically evaluated the fidelity of the probe in mouse (see Results).

Initially slices were dried at 37°C for 20 minutes and then postfixed 15 minutes at room temperature in 4% PFA in PBS. Autoclaved demineralizered DEPC-treated (0.1%) water (dH_2O) was used for all solutions. After washing, the slides were treated with a solution of 100 mM triethanolamine (pH 8.0) and 0.25% acetic anhydride in dH_2O. The sections were pretreated for 2–3 hours at 60°C in hybridization mix (50% formamide, 5× SSC, 1% or 5% Denhardts, 500 μg/mL salmon sperm DNA, 250 μg/mL yeast RNA) to minimize nonspecific binding of probe. The hybridization was initiated by heating the probe for 2 minutes at 90°C before adding it to a pre-

TABLE 1. Primary Antibodies Used

Antigen	Immunogen	Antibody details	Dilution used
Glycine	Glycine-paraformaldehyde-thyroglobulin	Immunosolution (Jesmond, Australia), rat polyclonal, IG1002	1:7,000
Green fluorescent protein (GFP)	GFP from *Aequorea Victoria*.	Abcam (Cambridge, UK), rabbit polyclonal, ab3751	1:2,000

warmed (60°C) hybridization mix. The concentration of DIG-labeled probe was 500 ng/mL. After adding the hybridization mix to the slides and covering them with Parafilm, the slides were placed overnight in a humidified chamber at 60°C. At the end of incubation the slides were rinsed twice with 1× SSC at 60°C, 1× SSC at 60°C (15 minutes), twice with 2× SSC at room temperature, 30 minutes with RNase (20 μg/mL) in 2× SSC at 37°C, 2× SSC at room temperature, 1× SSC at 60°C (1 hour), 0.2× SSC at room temperature. Nonspecific immunostaining was then blocked with 5% heat-inactivated normal goat serum for 30 minutes, after which the slides were incubated at 4°C in alkaline phosphatase-coupled anti-DIG antibody (Roche, Nutley, NJ; 1:2,000). The slides were then washed with a large volume of buffer (3 × 5 minutes). Prior to color development the slides were incubated in 5 mM levamisole. Development was carried out using 5 mM levamisole and BCIP/NBT (Roche) in buffer. The color reaction was allowed to develop in the dark for up to 12 hours at room temperature. The reaction was stopped by removing the developing mix by rinsing with PBS. The slices were then incubated for 5 minutes with Hoechst (1:2,000) or To-Pro-3 (1:10,000) in order to visualize nuclear DNA. Sense probes for GlyT2 and vGlut2 were used as controls and gave no signal (see also Lundfald et al., 2007).

To investigate the potential colocalization of GABA and glycine, GlyT2 in situ hybridization was performed in transgenic GAD67::eGFP mice. The sections were processed post-in situ with antibodies against GFP to reveal the GFP signal as described above (immunohistochemistry).

Microscopy

Images of TxRDA and immunohistochemically labeled sections were obtained using a Zeiss LSM 510 laser scanning microscope equipped with Argon 488 nm for excitation of Cy2 and GFP, a helium-neon 543 nm laser for excitation of Cy3 and Texas Red, and a helium-neon 633 laser for excitation of To-Pro-3. The respective filters used for detection were: 500–550 nm for Cy2 and GFP, 560–615 nm for Texas Red or Cy3, and 659–719 for To-Pro-3 and Cy5. The sections were scanned using 10× or 20× objectives and optical slices of 3 μm were obtained for separate channels obtained with a resolution of 1024 × 1024 (pixels per line × lines per frame). In each experiment a control section (without the secondary antibody) was used to measure the autofluorescence intensity. The photomultiplier gain was adjusted to a value below the autofluorescence emission level in order to subtract the part of the signal originating from the autofluorescence. Pictures were saved as individual TIFF files for later analysis in Adobe Photoshop (San Jose, CA).

Slides for in situ hybridization were viewed in a Nikon MicroPhoto-TX light microscope equipped with a fluorescent lamp and filter sets that allowed To-Pro-3 FITC and Texas Red excitation and detection. Using an AxoCam (Zeiss, Thornwood, NY) camera, photographs were first taken in normal light to detect the DIG-positive cells and then under fluorescent light to detect TxRDA or GFP. Images were obtained using the highest available resolution of the camera (3900 × 3090) and then saved as TIFF files for later analysis. When in situ hybridization was carried out in the GAD67::eGFP mice the confocal microscope's transmitted light channel, equipped with a photomultiplier, was used to obtain bright-field images of the situ hybridization. Subsequently, fluorescent images of TxRDA (CINs) and (GAD67-eGFP signal) were obtained using the settings described above.

For reproduction, image quality was improved in Adobe Photoshop using only brightness and contrast scaling.

Analysis

Counting of neuronal profiles was performed in Adobe Photoshop on high-resolution images of individual sections. Only neurons located in the ventral part of the spinal cord, where evidence for the location of the CPG has been clearly established (Kiehn and Kjaerulff, 1998), were included in the study. The ventral spinal cord was in this case defined as the part of the cord ventral to a horizontal line extending laterally from the dorsal border of the central canal (Fig. 1). For each neurotransmitter marker, counts were made in three to four different animals, in two to seven sections from each animal. Sections were taken more than 50 μm apart and spaced from the rostral to caudal end of the L2 segment. Neuronal profiles labeled with each of the neurotransmitter markers, TxRDA-labeled CIN profiles, and double-labeled profiles were identified using the zoom and multiple layer functions (see Fig. 3E). The Hoechst (light-microscopy images) or the To-Pro-3 (confocal images) staining was used to identify nuclei within each neuronal profile so that colocalization could be judged as real and not due to superimposition of neuronal profiles (see Fig. 3E). Any case in which more than one nucleus was evident within what appeared to be a single neuronal profile was discarded. Neuronal profiles were not counted within the smear of red fluorescence from TxRDA that was often seen near the midline, and which is probably due to contamination from TxRDA that may spread along the midline and central canal after application.

In each section we counted in the ventral spinal cord the total number of putative glycinergic, GABAergic or glutamatergic neuronal profiles, the total number of TxRDA-labeled CIN profiles, and the number of putative glycinergic, GABAergic, or glutamatergic CIN profiles. With these counts of neuron profiles we calculated the proportion of putative glycinergic, GABAergic, and glutamatergic CIN profiles relative to the entire ventral population of CIN-profiles and to the entire ventral populations of putative glycinergic, GABAergic, and glutamatergic neuronal profiles. Averages from all the sections from each animal were then averaged across animals to provide grand means ± standard deviations (SD). Hence, the present study estimates colocalization events that are normalized to counts of neuron profiles in the same sections (e.g., all the CIN profiles or all the glycinergic, GABAergic, or glutamatergic neuronal profiles), with the sections spaced so far apart that double counting neuronal profiles is impossible. The counting we provide is therefore aimed at giving relative proportions of identified neuronal profiles rather than absolute numbers of neurons in a given volume of the spinal cord. For convenience, we typically refer to neuronal profiles in the description below as neurons except when the quantitative data are presented.

Schematic section maps were drawn of each image and superimposed on a standard section outline to illustrate the relative positions of the different CIN phenotypes. We used the midline and the most ventral part of the section outline as reference landmarks for the alignment of sections. Although all sections came from the L2 segment in age-matched animals there was expected to be some variation in section size. We did not attempt to correct for this variation when super-

imposing the schematic maps (for example, by stretching or shrinking them). This means that the maps do not provide a precise quantitative but rather a qualitative assessment of relative neuron positions as obtained by the profile locations.

RESULTS

To include CINs that are putatively involved in coordinating locomotor movements, we focus our study on the upper lumbar (L) spinal cord, which in rodents has been shown to contain the most rhythmogenic part of the CPG (Kudo and Yamada, 1987; Cazalets et al., 1996; Kjaerulff and Kiehn, 1996; Cowley and Schmidt, 1997; Kremer and Lev-Tov, 1997; Bonnot et al., 1998, 2002; Kiehn and Kjaerulff, 1998; Gabbay et al., 2002; Christie and Whelan, 2005). Previous lesions studies have shown that all CINs that are involved in coordinating locomotor activity in the rodent are located in the ventral spinal cord (lamina VII, VIII, and X) and have their axons crossing in the ventral commissure (Kjaerulff and Kiehn, 1996; Nakayama et al., 2002). Consequently, to label such CINs we applied TxRDA to a longitudinal cut in the spinal cord ventral to the central canal along the entire length of the L2 segment (as defined by the ventral L2 rootlets leaving the spinal cord) (Fig. 1) and focused the analysis on CINs located in the ventral area. This CIN population includes both intrasegmentally and intersegmentally projecting CINs whose axons cross in the same segment as where their somata are located.

In initial experiments we applied TxRDA lateral to the midline (Fig. 1) in an attempt to avoid labeling of ipsilateral neurons that might have dendrites crossing or in close proximity to the midline. We then found that more CINs were labeled from midline than from parasagittal applications, and that the pattern and distribution of retrogradely labeled CINs were similar using the two protocols and similar to what has been reported in previous studies (Stokke et al., 2002; Nissen et al., 2005). For most of the experiments we therefore used midline applications (see below).

Putative glycinergic CINs

Initially we attempted to evaluate the glycinergic nature of CINs using antibodies against glycine. Although neuronal somata were well labeled using immunohistochemistry, the glycine immunoreactivity disappeared from somata in the ventral spinal cord (see Suppl. Fig. S1) after cutting CIN axons in the ventral commissure. Therefore, to visualize putative glycinergic CINs we used in situ hybridization against mRNA encoding the membrane-bound glycine transporter GlyT2. Of the two identified glycine transporters, GlyT1 and GlyT2, GlyT1 is mainly expressed in glial cells, whereas GlyT2 has been shown to be highly expressed in certain identified populations of glycinergic neurons (Poyatos et al., 1997; Zafra et al., 1997). The GlyT2 riboprobe we used for these experiments originated from a rat cDNA clone (Zafra et al., 1997) and it reliably labels putative glycinergic neurons in the brainstem (Stornetta et al., 2004). The rat GlyT2 gene shows 95% sequence overlap with the mouseGlyT2 gene (see Materials and Methods). To evaluate the fidelity of the in situ hybridization obtained with this probe in mouse we performed the following control experiments. First, glycine immunoreactivity (Allain et al., 2006) and GlyT2 in situ hybridization reactivity showed comparable patterns: intensive neuronal labeling in the deep dorsal horn (corresponding to lamina V–VII), and substantial labeling in the intermediate (laminae VII and X) and ventral (lamina VIII) spinal cord except for the motor nuclei in lamina IX (compare Fig. 2A,D; see also Allain et al., 2006). Second, we attempted to combine in situ hybridization for GlyT2 and immunohistochemistry for glycine to directly reveal colocalization. Unfortunately, the glycine antibody did not react in sections after in situ hybridization, making this approach impossible. We therefore performed in situ hybridization for GlyT2 in a transgenic mouse expressing the eGFP protein under the control of the GlyT2 promoter (Zeilhofer et al., 2005). We found an almost complete colocalization of GlyT2 in situ hybridization reactivity with eGFP immunoreactivity (Fig. 2A–C). Additionally, glycine immunohistochemistry colocalized perfectly with the GlyT2-eGFP-positive cells (Fig. 2D–F). Very few eGFP-positive cells were not glycine-immunoreactive (arrows Fig. 2D–F). We conclude from these experiments that the rat GlyT2 riboprobe efficiently labels putative glycinergic neurons in the ventral spinal cord of the mouse.

We then used this GlyT2 riboprobe to identify putative glycinergic CINs. Figure 3 shows transverse sections of one side of the L2 ventral spinal cord with retrogradely labeled CINs (Fig. 3A), GlyT2 mRNA-positive neurons (Fig. 3B), and Hoechst-stained nuclei (Fig. 3C). The photos are superimposed in Figure 3D with arrows pointing to CINs that were GlyT2 mRNA-positive. Figure 3E shows a GlyT2 mRNA-positive and a GlyT2 mRNA-negative CIN in enlargements.

When the relative locations of the putative glycinergic CINs is plotted separately for midline versus parasagittal labeling protocols, the picture appears quite similar, with neurons distributed throughout the ventral spinal cord with no obvious mediolateral or dorsoventral clustering (Fig. 3F: midline; Fig. 3G: parasagittal). The proportion of CIN profiles that were GlyT2 mRNA-positive was about one-third in both of the retrograde labeling protocols (midline labeling: 30% ± 5% [n = 3], Fig. 3H, first bar; parasagittal labeling: 27% ± 3.7% [n = 3], Fig. 3G, third bar). The proportion of GlyT2 mRNA-positive neuron profiles that were CINs was also about one-third (27% ± 5.3% [n = 3] using midline labeling, Fig. 3H, second bar; 32% ± 2.4% [n = 3] using parasagittal labeling, Fig. 3H, fourth bar). When we compared the number of double-labeled neuron profiles in the two labeling protocols they were very similar (midline labeling: 40 ± 8.0; parasagittal: 33 ± 4.9). In all of the following experiments we only used the midline application protocol for retrograde labeling.

Putative GABAergic CINs

GABA is synthesized by the enzyme GAD, which is found in two isoforms, GAD65 and GAD67. The presence of one or the other or both of these enzymes, particularly in synaptic terminals, is considered a good indicator of a GABAergic phenotype. However, whereas antibodies against GAD65 and GAD67 label axon terminals strongly the same antibodies fail to label neuronal somata in the rodent spinal cord (Mackie et al., 2003; Weber et al., 2007). To reveal putative GABAergic CINs we therefore used transgenic mice that express eGFP under control of the GAD65 promotor (Hughes et al., 2005), or knockin mice with eGFP in the GAD67 gene (Tamamaki et al., 2003). Both of these mice reliably express eGFP in certain identified populations of GABAergic neurons, and we therefore used them here to provide an indication of which ventral CINs may be GABAergic.

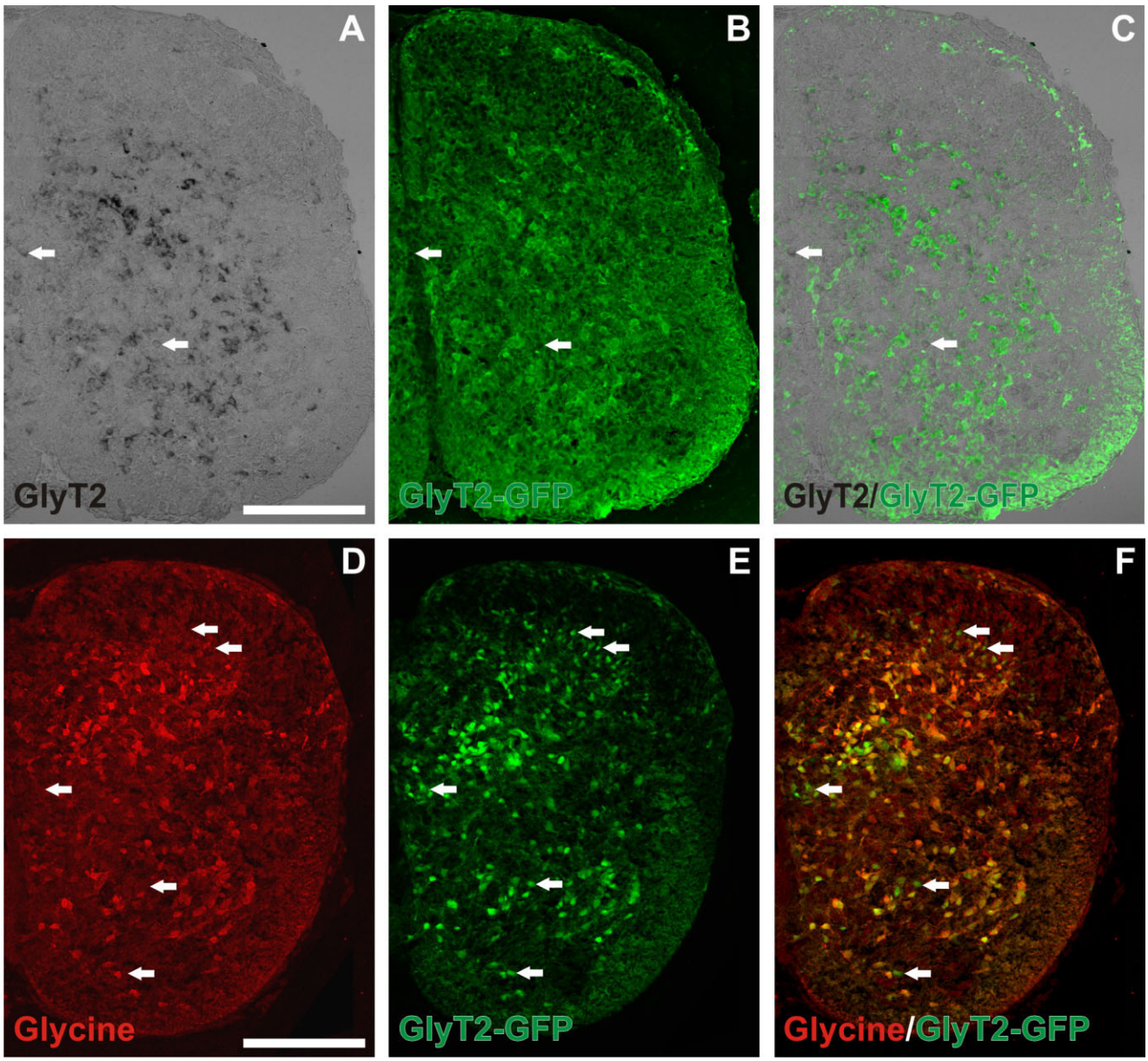

Figure 2.
In situ hybridization for GlyT2 mRNA **(A–C)** and immunohistochemistry for glycine **(D–F)** show the same degree of colocalization with GFP in a transgenic GlyT2::eGFP mouse. A: Transverse section of L2 showing GlyT2 in situ hybridization (black) in a GlyT2::eGFP mouse. B: View of the same section as in A after immunohistochemistry for eGFP (green). C: Overlay of A and B showing almost perfect colocalization of GlyT2 mRNA and eGFP in neuron somata. The arrows point to the few exceptional somata that showed hybridization for GlyT2 mRNA but were negative for eGFP protein. D: Transverse section of L2 immunostained with an antibody against glycine (red) in a GlyT2::eGFP mouse. E: Native GlyT2-eGFP fluorescence (green) in the same section as in D. F: Overlay of D and E showing an almost perfect co-localization of glycine immunostaining and the eGFP. Arrows point to a few eGFP-positive, glycine-negative somata. A magenta-green copy is available as Supplementary Figure 2. Scale bars = 200 μm.

In the GAD65::eGFP mice, virtually all eGFP-positive neurons were confined to the dorsal horn with somata spread throughout the superficial (I–III) and deep (IV–V) laminae, with a particularly high density in the medial parts of the deep laminae (Fig. 4A). Only a few scattered GFP-positive neurons were present in the ventral spinal cord, and these showed little or no overlap with retrogradely labeled CINs (Fig. 4B) (see Discussion). By contrast, the GAD67::eGFP mice contained a more widely distributed population of eGFP-positive neurons throughout the dorsoventral extent of the spinal cord (Fig. 4C). GAD67-eGFP-positive neurons were abundant in the superficial laminae of the dorsal horn (laminae I–III) and medially in laminae IV–VI. GAD67-eGFP-positive neurons were scattered throughout the ventral spinal cord, with the exception of the lateral motor nucleus (lamina IX), and with a higher density in the most medial part of the ventral spinal cord. Lamina X in

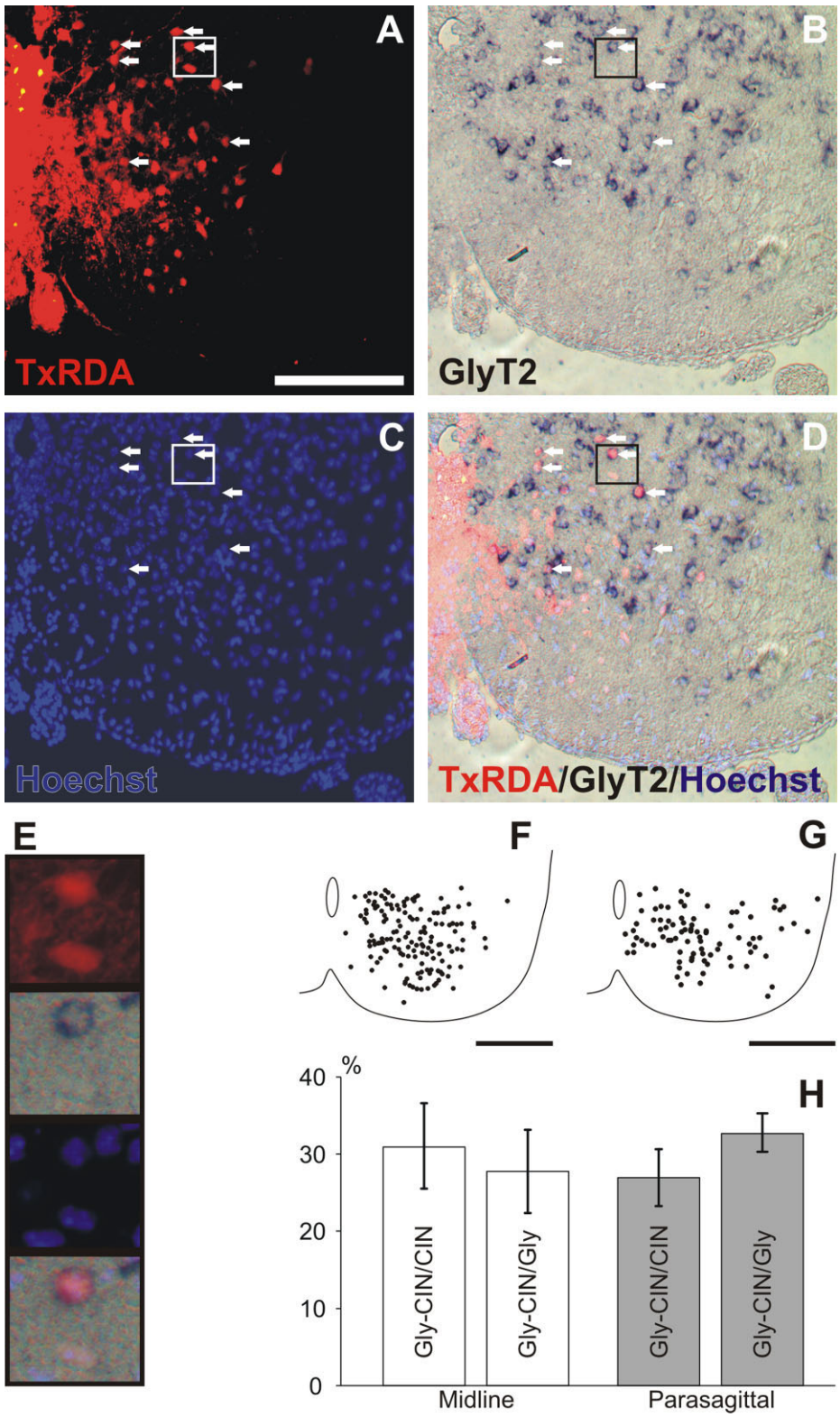

Figure 3.
Detection of putative glycinergic CINs in the ventral mouse spinal cord. **A:** CINs in the ventral spinal cord of a transverse section from L2 retrogradely labeled with TxRDA (red) applied to the midline. **B:** Putative glycinergic neurons identified by in situ hybridization against GlyT2 mRNA (purple) in the same section. **C:** Hoechst labeling of nuclei (blue) in the same section. **D:** Merged view of A–C showing GlyT2 mRNA-positive CINs. **E:** Enlargements from A–D (box areas) showing identification of Glyt2 mRNA-positive and Glyt2 mRNA-negative neurons. **F:** Cumulative plot of GlyT2 mRNA-positive CINs from three sections in each of three animals where CINs were retrogradely labeled by applying TxRDA to a midline cut. **G:** Cumulative plot of GlyT2 mRNA-positive CINs from three sections in each of three animals where CINs were retrogradely labeled by TxRDA applied to a parasagittal cut. **H:** The percentage of CINs that are GlyT2 mRNA-positive (first and third bar) and the percentage of GlyT2 mRNA-positive neurons that are CINs (second and fourth bar) are shown for the midline (white) and parasagittal (gray) labeling protocols. Scale bar = 200 μm.

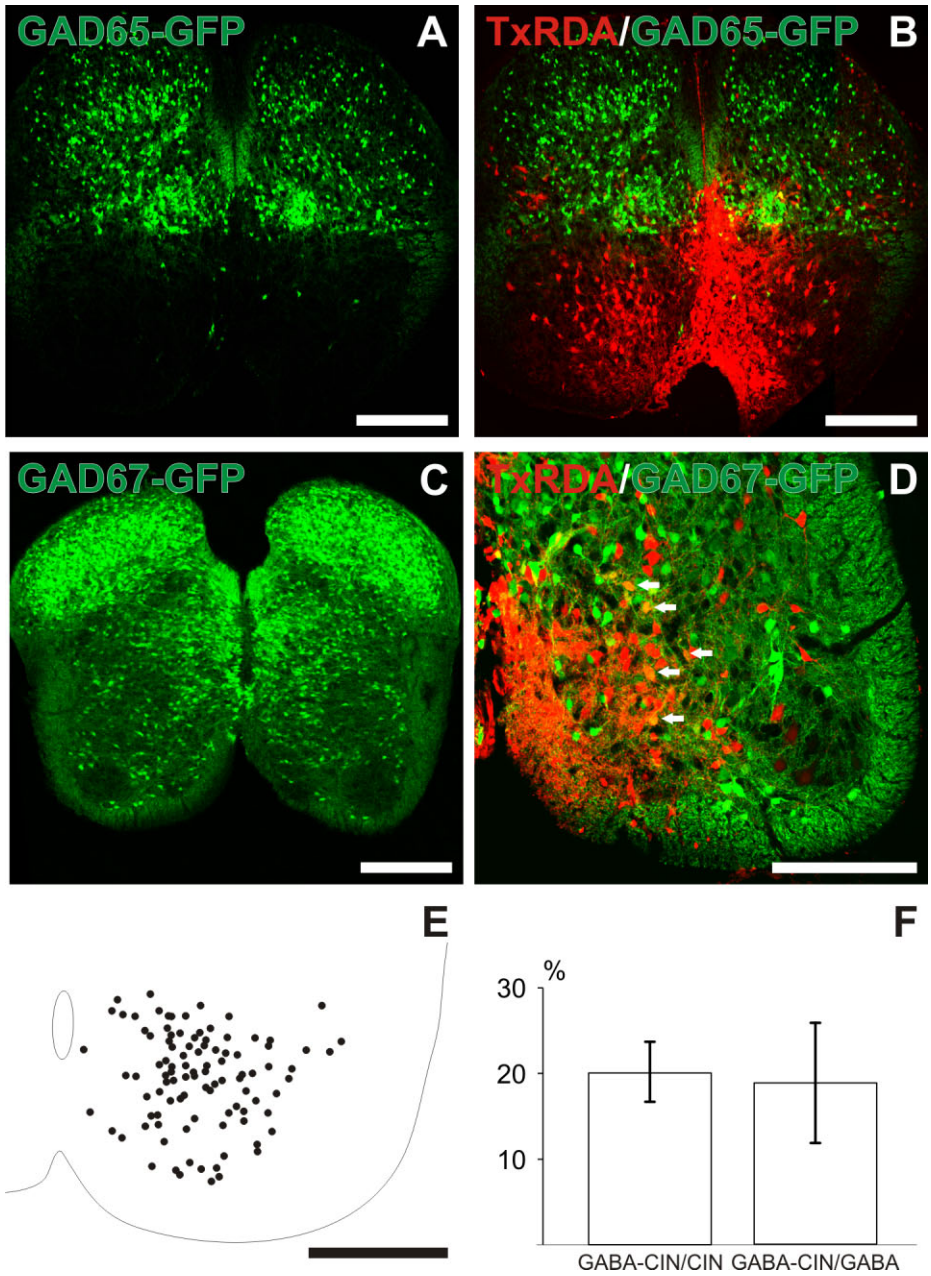

Figure 4.
Detection of putative GABAergic CINs in the ventral mouse spinal cord. Putative GABAergic neurons were visualized using transgenic mice that express eGFP under the promoters for one of the two GABA synthesizing enzymes GAD-65 **(A,B)** and GAD-67 **(C,D)**. A: Transverse section from L2 showing eGFP-positive neurons in the GAD65::eGFP mouse. Note that there are hardly any eGFP-positive neurons in the ventral cord. B: TxRDA retrogradely labeled CINs (red) in a transverse section of L2 from a GAD65::eGFP mouse (green, eGFP). Native eGFP fluorescence. C: Transverse section from L2 showing eGFP-positive neurons in the GAD67::eGFP mouse. Note the widespread distribution of eGFP-positive neurons both dorsally and ventrally. D: TxRDA retrogradely labeled CINs (red) in a transverse section of L2 from a GAD67::eGFP mouse (green, eGFP). Native eGFP fluorescence. **E:** Cumulative plot of GAD67-eGFP-positive CINs from three sections in each of three animals in which CINs were retrogradely labeled from the midline. **F:** The percentage of retrogradely labeled CINs that are GAD67-eGFP-positive (first bar) and the percentage of GAD67-eGFP-positive neurons that are CINs (second bar). A magenta-green copy is available as Supplementary Figure 3. Scale bars = 200 μm.

particular was always strongly populated by GAD67-eGFP-positive neurons. Particularly bright GAD67-eGFP-positive neurons were seen medial to the lateral motor neurons. These latter neurons have been shown to be Renshaw cells (Nishimaru et al., 2005; Alvarez et al., 2005; Nishimaru et al., 2006). The ventrally located GAD67-eGFP-positive cells intermingled with CINs (Fig. 4D) and a fraction was CINs (Fig. 4D–F). GAD67-eGFP-positive CINs were located mainly in laminae VII and VIII, but a very few were found in the most lateral part of lamina VII (Fig. 4E). The proportion of CIN profiles that were

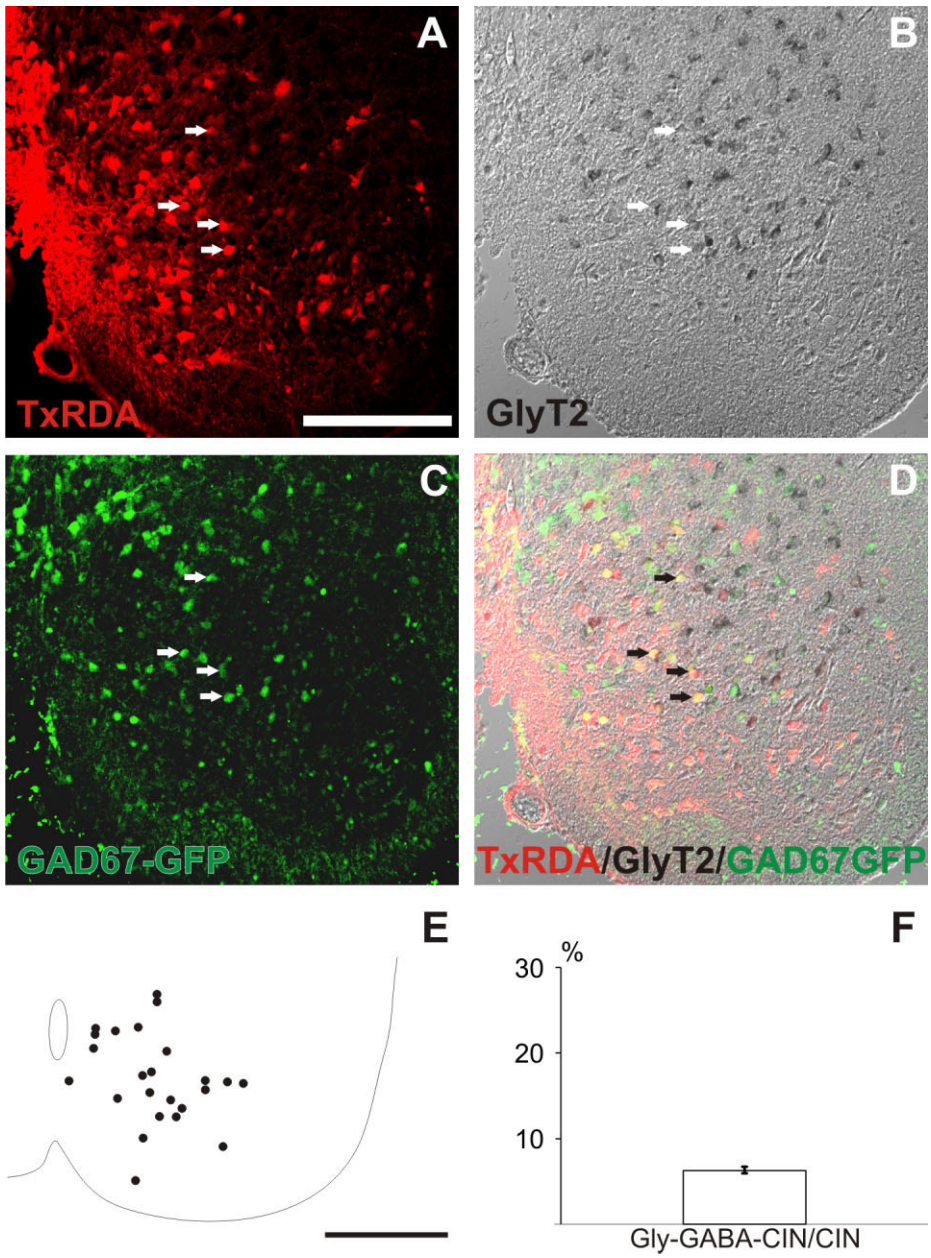

Figure 5.
Detection of putative combined glycinergic/GABAergic CINs in the ventral mouse spinal cord. **A–C:** Transverse section from L2 showing retrogradely labeled CINs. TxRDA applied to a midline cut (A), in situ hybridization against GlyT2 mRNA (black) (B), and GAD67-eGFP expression (green) (C). **D:** Overlay of A–C. The arrows point to triple-labeled cells. **E:** CINs positive for both GAD67-eGFP and GlyT2 mRNA plotted from three sections in each of three animals where CINs were retrogradely labeled from the midline. **F:** The percentage of all labeled CINs that are GAD67-eGFP-positive and GlyT2-eGFP-positive. A magenta-green copy is available as Supplementary Figure 4. Scale bar = 200 μm.

GAD67-eGFP-positive was 20 ± 3.38% (n = 3, Fig. 4F, first bar), and the proportion of GAD67-eGFP-positive neuronal profiles that were CINs was 18 ± 7%, (n = 3, Fig. 4F, second bar).

Putative combined GABAergic-glycinergic CINs

Cotransmission of GABA and glycine has been documented in the spinal cord (Jonas et al., 1998), and colocalization of GABA and glycine is particularly prominent in the spinal cord embryonically and early postnatally (Jonas et al., 1998; Allain et al., 2006). We therefore assessed the colocalization of these transmitters in CINs by using in situ hybridization for GlyT2 mRNA in the GAD67::eGFP mice.

Figure 5A–D shows transverse sections of one side of the L2 ventral spinal cord with retrogradely labeled CINs (Fig. 5A), in situ labeling of GlyT2 mRNA-positive neuron (Fig. 5B), and

GAD67-eGFP-positive neuron (Fig. 5C). The photos are superimposed in Figure 5D with arrows pointing to CINs that are both GlyT2 mRNA-positive and GAD67-eGFP-positive. These are restricted to the most medial part of layers VII and VIII and are absent from lamina X (Fig. 5E). The percentage of CIN profiles in the ventral spinal cord that were both GAD67-eGFP- and GlyT2 mRNA-positive was 6 ± 0.28% (n = 3, Fig. 5F). In general, these putative GABAergic/glycinergic CIN profiles were distributed in a similar pattern to that of the putative GABAergic CINs, with a somewhat higher density medially than laterally.

Putative glutamatergic CINs

We used in situ hybridization against vGluT2 mRNA in combination with retrograde labeling to visualize putative glutamatergic CINs. Previous experiments from our group and others have shown that among the three known vesicular glutamate transporters 1–3 (vGluT1–3) selectively expressed in glutamatergic neurons, vGluT2 is the dominant transporter expressed in neurons in the ventral part of the mouse and rat spinal cord (Kullander et al., 2003; Oliveira et al., 2003; Herzog et al., 2004; Wilson et al., 2005; Lundfald et al., 2007). VGluT1 transcripts are mainly expressed in somata in the medial part of dorsal spinal cord (Oliveira et al., 2003; Kullander et al., 2003; see, however, Herzog et al., 2004) and the dorsal root ganglion cells, and vGluT3 transcripts are not detected in the ventral spinal cord at all or in very few neurons (Oliveira et al., 2003).

In accordance with previous observations (Lundfald et al., 2007; Crone et al., 2008), we found intensely labeled vGluT2-positive neurons in laminae VII, VIII, and X, although the density appeared to be lower in the lateral part of layer VII (Fig. 6B,D). Faintly labeled neurons were also seen in lamina X (Herzog et al., 2004; Nishimaru et al., 2005). vGluT2-positive CINs (Fig. 6C,D) were present throughout the ventral spinal cord (except for the motor nucleus), with a somewhat lower density in the lateral part of the cord (Fig. 6D). The distribution of the putative glutamatergic CINs was similar to that of the putative glycinergic CINs (Fig. 6D, compare to Fig. 3E,F). The percentage of retrogradely labeled CIN profiles that expressed vGluT2 mRNA was 26 ± 0.67% (n = 3, Fig. 6E, first bar) and the percentage of vGluT2 mRNA-positive neuronal profiles that were CINs was 22 ± 2.3% (n = 3, Fig. 6E, second bar).

DISCUSSION

Spinal CINs play an essential role in coordinating rhythmic motor activity between the left and right sides of the body during locomotion. From physiological studies in mammals it is known that this coordination involves glycinergic, GABAergic, and glutamatergic crossed connections. In the present study we describe anatomically the relative proportions and distributions of putative glycinergic, GABAergic, combined glycinergic/GABAergic, and glutamatergic CINs in the locomotor region (laminae VII, VIII, and X) of the lumbar spinal cord in the newborn mouse.

Our study shows that the putative glycinergic, GABAergic, and glutamatergic phenotypes are found in comparable numbers whereas a smaller proportion of CINs may have a combined glycinergic/GABAergic phenotype. There was no particular differential distribution of these different CIN phenotypes in the ventral spinal cord, aside from a somewhat more medial distribution of putative GABAergic CINs relative to the others. Our data suggest that in addition to the glycinergic CINs that constitute the core of the left–right coordinating circuits in locomotor models of aquatic vertebrates, the rodent CPG may encompass equally strong GABAergic and glutamatergic left–right coordinating circuits.

Technical considerations

Unlike glutamatergic neurons, where the presence of functional vesicular transporter proteins (e.g., vGluT2), is considered an indicator of a glutamatergic phenotype, GABAergic and glycinergic neurons share the same vesicular inhibitory amino acid transporter, VIAAT (Wojcik et al., 2006). Therefore, establishing the presence of either of these transmitter phenotypes anatomically requires a differential evaluation of specific characters, such as synthesizing enzymes (GAD65/67) or reuptake transporters (GlyT2). There are also excellent antibodies against GABA and glycine that label neuronal somata (Storm-Mathisen et al., 1983; Allain et al., 2006). Unfortunately, glycine immunoreactivity was drastically weakened in the neonatal spinal cord by the axotomy required to retrogradely label the CINs. This change in immunoreactivity occurred already after 2–3 hours and was substantial after 5–7 hours. Similar findings have been described for choline acetyltransferase and vesicular acetylcholine transporter immunoreactivity in chronically axotomixed cholinergic neurons (Rende et al., 1995; Matsuura et al., 1997). The depletion of glycine immunoreactivity was not a consequence of the in vitro incubation because this did not occur in nonaxotomized interneurons in the same sections.

We were therefore forced to use methods other than glycine and GABA immunohistochemistry to identify putative GABAergic and glycinergic CINs in the present study. Antibodies against the GABA-synthesizing enzymes GAD65 and GAD67 or against the neuronal glycine transporter GlyT2 also typically gave poor labeling of neuronal somata in the neonatal mouse and rat spinal cord (unpubl. obs.), presumably because the proteins are localized principally in synaptic terminals. To visualize putative inhibitory CIN somata directly we therefore used transgenic animals that express eGFP under the control of GAD65 or GAD67 promoters (GABA) and in situ hybridization against GlyT2 mRNA (glycine). In the case of the GAD65::GFP mice there was a complete absence of eGFP-positive neurons in the ventral horn, precluding the identification of any GAD65-positive CINs. This absence may reflect a relative difference in the expression levels of the two GAD enzymes. Although GAD65 and GAD67 have been reported to be coexpressed in most GABAergic neurons in the adult, GAD67 mRNA levels are generally higher than GAD65 mRNA levels in the spinal cord, especially in the ventral horn (Ma et al., 1994; Feldblum et al., 1995). When evaluated at the protein level, GAD67 is always expressed at higher levels than GAD65 throughout the spinal cord (Mackie. et al., 2003). Since the relative difference is seen at the level of transcripts as well as protein, the expression of eGFP driven by the GAD65 promoter may be expected to be similarly low in the ventral spinal cord compared to that of eGFP driven by the GAD67 promoter.

The best indication of potential GABA synthesis in ventral spinal CINs was therefore obtained in the GAD67::eGFP mice. The specificity of eGFP expression in the GAD67::eGFP mouse has been previously evaluated in the brain and spinal cord using in situ hybridization for GAD67 showing a perfect match between eGFP and GAD67 expression (Tamamaki et al., 2003) and a

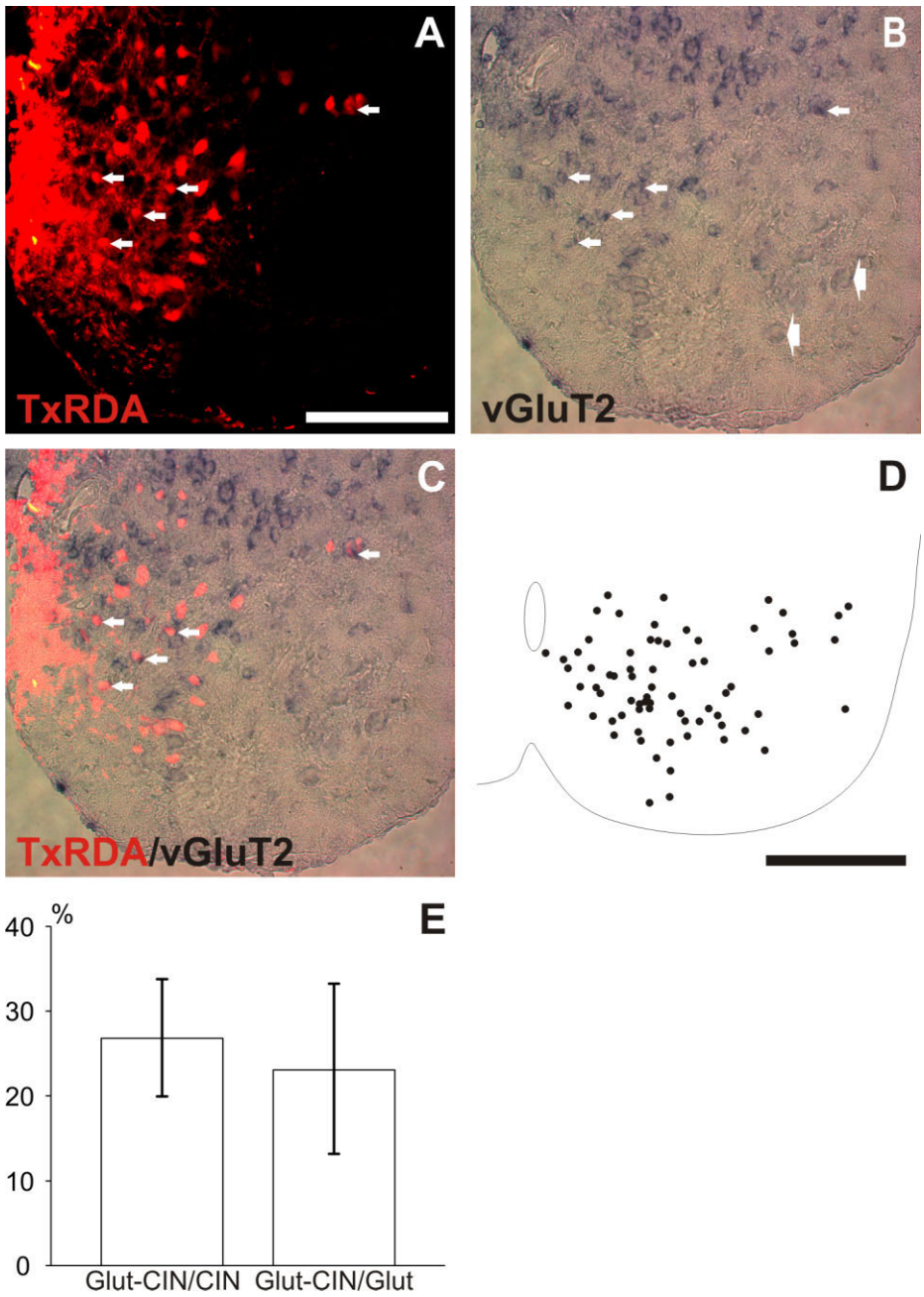

Figure 6.
Detection of putative glutamatergic CINs in the ventral mouse spinal cord. **A:** Transverse section of ventral L2 spinal cord showing CINs retrogradely labeled with TxRDA from the midline. **B:** In situ hybridization against vGluT2 mRNA (purple) in the same section. Broad arrows show faint labeling of putative motor neurons. **C:** Overlay of A and B. The white arrows point to putative glutamatergic CINs. **D:** Plot of vGluT2 mRNA-positive CINs based on at least three sections from each of three animals where CINs were retrogradely labeled from the midline **E:** The percentage of all labeled CINs that are vGluT2 mRNA-positive (first bar) and the percentage of vGluT2 mRNA-positive neurons that are CINs (second bar) in the ventral spinal cord. Scale bars = 200 μm.

distribution corresponding closely to the pattern of expression of GAD67 found by others (Ma et al., 1994). In electrophysiological recordings we have also shown directly that eGFP-positive cells in this mouse release GABA (unpubl.).

Glutamatergic CINs were visualized by in situ hybridization against vGluT2, which is the dominant vesicular transporter in the ventral spinal cord of mice (Lundfald et al., 2007; Crone et al., 2008). The specificity of the vGluT2 riboprobe used in this study has been previously evaluated (Lundfald et al., 2007). Since excessive developing times (>30 hours) with BCIP/NBT may result in unspecific labeling, we took great care to keep developing times as short as possible (6–24 hours), thereby

TABLE 2. Summary of CIN Phenotypes in Rodents

Anatomy	Mouse[1]: Percentage in relationship to the total population of labeled CINs	Mouse[1]: Percentage in relationship to the population of transmitter-identified CINs	Rat[2]: Percentage in relationship to the total population of labeled CIN terminals	Rat[2]: Percentage in relationship to the population of transmitter-identified CIN terminals
Glycine	20%	30%	27%	32%
GABA	14%	21%	14%	17%
Glycine/GABA	6%	9%	16%	19%
Total inhibitory	40%	60%	58%	69%
Glutamate	26%	39%	27%	31%
Unknown	35%	0%	15%	0%
Total	100%	100%	100%	100%

Electrophysiology	Mouse[3]: Percentage in relationship to the total population of labeled CINs	Mouse[3]: Percentage in relationship to the population of transmitter-identified CINs	Rat[4]: Percentage in relationship to the total population of labeled CINs	Rat[4]: Percentage in relationship to the population of transmitter-identified CINs
Inhibitory	11%	30%	17%	24%
Excitatory	33%	70%	55%	77%
Unknown	47%	0%	28%	0%
Total	100%	100%	100%	100%

[1]Present study.
[2]Weber et al., 2007.
[3]Quinlan and Kiehn, 2007.
[4]Butt and Kiehn, 2003.

avoiding any background signal in our preparations. The weak vGluT2 mRNA expression in motor neurons has been observed previously and may be explained by the corelease of glutamate from motor neurons in early postnatal animals (Mentis et al., 2005; Nishimaru et al., 2006).

In the case of the GlyT2 riboprobe, specificity is supported by colocalization with glycine immunoreactivity and with eGFP immunoreactivity in the transgenic GlyT2::eGFP mice.

Retrograde labeling did not diminish the vGluT2 and GlyT2 mRNA signals or the eGFP immunoreactivity, as it did glycine immunoreactivity, suggesting that axotomy has less effect on the stability of these transcripts than on the neurotransmitters themselves.

We conclude that the combination of phenotypic markers used here provides a means to specifically distinguish putative glutamatergic, GABAergic, and glycinergic phenotypes in retrogradely labeled spinal CINs. However, although several of the markers involved have been correlated with the physiological utilization of the respective transmitter in certain neuronal systems, they cannot be considered definitive markers of neurotransmitter phenotype in the absence of physiological confirmation. First of all, neither the use of reporter genes driven by regulatory elements for enzymes or transporters nor the use of in situ hybridization to detect mRNA for transporters provides any direct information about the degree of protein expression because posttranscriptional regulatory events may affect the level of expression of protein. Moreover, even if the relevant proteins were detected immunohistochemically in neuronal somata, this would not be proof that they were functional or properly localized to generate neurotransmitter release within the synapse. For these reasons we have decided to exercise caution by referring to the phenotypes as putative neurotransmitter phenotypes, with the anticipation that the advantages of the neonatal mouse spinal cord preparation will permit a physiological confirmation of many of these phenotypes in the future.

Although the phenotyping appears to be specific, it clearly does not account for all of the retrogradely labeled CINs. Thus, the sum of putative inhibitory and excitatory CIN phenotypes is not 100% but only 70%. This is similar to what has been found for CIN synaptic terminal phenotyping in the rat (85%; Weber et al., 2007) and the cat (67%; Bannatyne et al., 2003; Jankowska et al., 2009) (see below). One possible explanation for the discrepancy is that the remaining CINs may express other neurotransmitters. In adult cat there is indeed a small number of cholinergic neurons with commissural projections (Huang et al., 2000) and it is possible that this group of neurons also exist in the neonatal mouse and may account for a proportion of unidentified CINs. Another possibility is that CINs utilizing peptide neurotransmitters account for some of the shortfall (Ryge et al., 2008), which we did not test for here. We cannot exclude such alternative transmitters, but we feel that a more likely explanation for the deficit in our study is that neither the RNA (detected by the in situ hybridization) nor the eGFP protein in the transgenic mice is expressed in sufficient levels in all the neurons to be detected by the techniques used. Presumably, neurons missing for this reason would be equivalently distributed among the different phenotypes and therefore would not change the relative spatial distributions or proportions. Therefore, to facilitate the comparison of our data with other anatomical and electrophysiological studies of CIN distributions in mammals we will hereafter express CIN transmitter phenotypes as proportions relative to the population of transmitter-identified CINs rather than as proportions relative to the total population of retrogradely labeled CINs (Table 2).

Organization of ventrally located CINs in the rodent

In the present study we find that putative glycinergic and GABAergic CINs comprise about 60% of the transmitter-identified CINs in the ventral spinal cord, while the remainder comprises putative glutamatergic CINs (Table 2, column 2). CINs expressing only glycinergic markers (30%) are slightly more abundant than those expressing only GABAergic markers (21%). The putative glycinergic and GABAergic pheno-

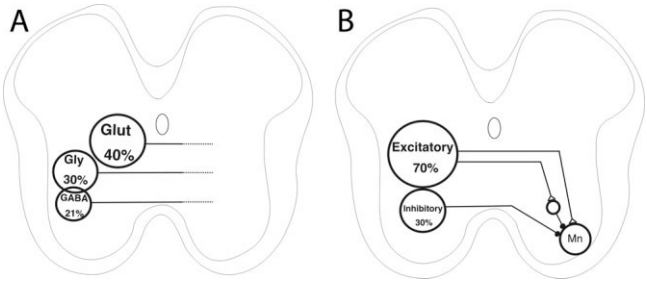

Figure 7.
Schematic diagram of the relative proportions of transmitter-identified CINs obtained anatomically **(A)** and electrophysiologically **(B)** (see text for details). Note that the schematic representation in this diagram does not reflect the relative position of the CINs populations in the ventral spinal cord.

types appear to be coexpressed in only a minor population of the transmitter-identified CINs (9%). These proportions are similar to proportions obtained from phenotyping synaptic terminals in the newborn rat spinal cord, in a study where anterogradely labeled CIN terminals in the ventral horn were analyzed using antibodies against glycinergic, GABAergic, and glutamatergic presynaptic neurotransmitter markers (GAD65/GAD67 for GABA, GlyT2 for glycine, vGluT1-2 for glutamate; Weber et al., 2007). That study showed that putative inhibitory CIN synaptic terminals constitute 69% of all the phenotyped CIN terminals (Table 2, column 4). CIN synaptic terminals expressing purely glycinergic or GABAergic markers constituted 32% and 17% of all phenotyped CIN terminals, respectively, whereas glycinergic and GABAergic markers colocalized in 19% of the phenotyped CIN terminals. These data cannot be directly compared to our results because it is not known if the different CIN transmitter classes make equal numbers of synapses on contralateral target neurons, but the comparison suggests an overall picture that is similar in the neonatal mouse and rat.

Populations of rodent CINs have also been transmitter-phenotyped through electrophysiological sampling by assessing direct or indirect synaptic effects on motor neurons. This has been done for the CIN population in the ventral spinal cord that projects intrasegmentally (in the same segment) in neonatal mice (Quinlan and Kiehn 2007; L2–L3 projecting) and for the CIN population that projects intersegmentally from the upper lumbar spinal cord (L2) to motor neurons located in lower lumbar spinal cord (L4–L5), so-called L2 descending CINs, in neonatal rats (Butt and Kiehn, 2003). These CIN pathways to motor neurons are organized in 1) a dual inhibitory system composed of monosynaptically projecting glycinergic/GABAergic CINs and glutamatergic CINs that mediate inhibition through local inhibitory interneurons, and 2) a single excitatory system of glutamatergic CINs that excite motor neurons. When comparing the relative contribution of phenotypes obtained by electrophysiological sampling of CINs with the data obtained from the anatomical sampling here the results appear very different (Fig. 7). Thus, in the electrophysiological studies most of the CINs were determined to be glutamatergic both for intrasegmental (Quinlan and Kiehn, 2007) and for intersegmental (Butt and Kiehn, 2003) connections (33% of the total population or 70% of the transmitter-identified CINs in the mouse and 55% of the total population or 77% of the transmitter-identified CINs in the rat; Table 2, columns 6 and 8) (Fig. 7). This predominance of excitation does not seem to be the result of GABA having a depolarizing effect at neonatal stages because glutamatergic receptor antagonists blocked the excitatory CIN effects in the electrophysiological experiments. Moreover, the GABAergic CINs could be defined pharmacologically in the electrophysiological experiments and had a hyperpolarizing effect on motor neurons (Butt and Kiehn, 2003; Quinlan and Kiehn, 2007). Additionally, we have seen that Renshaw cells that express GAD67::eGFP in the early postnatal period can hyperpolarize motor neurons when activated (unpubl. data from Ole Kiehn's laboratory).

The most likely explanation for the discrepancies between our anatomical study and the electrophysiological studies is that they sample different pools of CINs. The entire population of CINs in the L2 segment is labeled by the midline tracer injections used here, whereas only those CINs that have direct or indirect synaptic connections to motor neurons are detected electrophysiologically (Fig. 7). The electrophysiological sampling of motor neurons therefore excludes CINs that terminate exclusively on interneurons, whereas the population of CINs labeled retrogradely from the midline includes CINs that project to motor neurons as well as to interneurons only (Birinyi et al., 2003; Matsuyama et al., 2004, 2006). This condition seems to leave a relatively large proportion of CINs unidentified in electrophysiological studies—especially when it comes to segmental circuits (Quinlan and Kiehn, 2007)—and to skew the relative CIN relationship in the electrophysiological data toward an excitatory predominance. The anatomical data presented here, therefore, provide a more complete picture of the overall CIN population in the ventral spinal cord and include CINs that may not be functionally involved in the regulation of locomotion. Indeed, not all CINs are rhythmically active during locomotor activity (Butt et al., 2002; Butt and Kiehn, 2003; Zhong et al., 2006).

Together, the anatomical data suggest that both glycinergic and GABAergic CIN systems may play major roles in coordinating left–right motor activity in rodents. Both the anatomical and electrophysiological data are consistent with a situation in which glutamatergic CINs contribute significantly to crossed activity and dominate glycinergic and GABAergic CINs at the motor neuronal level. This skewed distribution at the motor neuron level suggests that many of the putative glycinergic and GABAergic CINs identified here project exclusively to interneurons and suggest that CIN populations projecting to motor neurons and interneurons might have different phenotypic compositions. Moreover, the relatively low rate of coexpression of glycinergic and GABAergic markers suggest that the two inhibitory CIN transmitter pathways for the most part can be controlled independently.

Comparison to CIN systems in other vertebrates

The transmitter phenotypes of spinal CINs have been anatomically characterized in a number of other vertebrate species. In the adult cat spinal cord, a small number ($n = 16$) of CINs located in laminae VI, VII, and VIII were transmitter-phenotyped after intracellular biotin filling using antibodies against glycinergic, GABAergic, and glutamatergic presynaptic neurotransmitter markers (GAD65/GAD67, GlyT2, vGluT2) (Bannatyne et al., 2003; Jankowska et al., 2009). Three of these CINs had synaptic terminals that were GlyT2-positive or were in close apposition to glycinergic postsynaptic com-

plexes, whereas 13 CINs had vGluT2-positive terminals. Thus, in this small sample, of the phenotyped CINs, those that were putatively inhibitory were glycinergic and made up a small percentage (19%) of the CINs, whereas those that were putatively excitatory made up a large majority (81%) of the CINs. CINs located in laminae VI–VII were all putative excitatory, whereas CINs located in lamina VIII represented a mixture of putative glycininergic and glutamatergic CINs (40% and 60%, respectively). We found no sign of such a differential laminar distribution of CIN neurotransmitter phenotypes in the neonatal mouse in the present study. Using retrograde tracing in combination with immunohistochemistry in the adult lamprey ≈65% of the total population of phenotyped CINs was found to be putatively glycinergic, whereas the remaining CINs were putatively glutamatergic (Mahmood et al., Eur J Neurosci, submitted). In the embryonic zebrafish the putative transmitter phenotypes of anatomically defined spinal CINs have been characterized using transgenic fish that express eGFP under the control of genes for glycinergic, GABAergic, and glutamatergic marker proteins (Higashijima et al., 2004a,b). By comparing the results of this transmitter phenotyping with the different classes of CINs in the zebrafish spinal cord it has been calculated that ≈35% of spinal CINs (including ventral and dorsal CINs) are glycinergic, whereas the remaining 65% are glutamatergic (Fetcho, 1990; Higashijima et al., 2004a,b; Nissen et al., 2008). In the tadpole embryo there are no reports of excitatory CINs and all CINs appear to be glycinergic (Dale et al., 1986; Roberts, 2000).

From this comparison it is clear that, with the notable exception of the *Xenopus* tadpole, all investigated species have both inhibitory (glycinergic and/or GABAergic) and excitatory (glutamatergic) CIN populations in the cord. However, the relative sizes of putative inhibitory and excitatory CIN populations vary. The strong GABAergic component of the CIN system found in rodents clearly deviates from what is found in all other vertebrates investigated. The GABAergic component might be an early developmental phenotype in mammals that is replaced by a purely glycinergic component later in adult life. The difference between neonatal rodents and the aquatic vertebrates, however, seems not to reflect a developmental difference but rather a fundamental difference in spinal cord organization, since putative GABAergic CINs were absent both in zebrafish embryos, *Xenopus* tadpoles, and lamprey adults. Together, the comparison of the reported data suggests that most vertebrate phyla independent of their developmental stage use a combined inhibitory and excitatory CIN system to coordinate left–right spinal cord activity. It should be noted that we are aware that comparing different species and developmental stages is not straightforward. For example, the fully independent autonomy of movements observed at early developmental stages in *Xenopus* larvae and zebrafish do not have a counterpart in mammals. Thus, although the some of the CIN populations so far identified in fish or frog may be evolutionarily conserved, others might belong to a species-specific repertoire.

Functional considerations of CIN organization in vertebrate CPGs

Physiologically, most species so far investigated have both inhibitory (glycinergic) and excitatory (glutamatergic) crossed projections within the locomotor CPG, the former mediating left–right alternation and the latter mediating left–right synchrony (Buchanan and Cohen, 1982; Dale, 1985; Bracci et al., 1996; Cazalets et al., 1996; Cowley and Schmidt, 1997; Roberts, 2000; Grillner, 2003; Hinckley et al., 2005). However, in rodents it has been shown that segmental crossed inhibition is not only mediated by glycinergic CINs but also indirectly by excitatory CINs connecting through inhibitory interneurons located on the contralateral side (Quinlan and Kiehn, 2007). This segmental dual inhibitory system may also be present in the cat (Jankowska, 2008; Kiehn et al., 2008). Recent experiments from the lamprey have also shown that the CPG controlling fin movements contains a dual inhibitory pathway (Roberts, 2000; Mentel et al., 2006), suggesting that such a dual inhibitory CIN system might have evolved to control limb or limb-like (fin) movements. In addition, electrophysiological studies (Quinlan and Kiehn, 2007) and this study show that putative GABAergic CINs also constitute part of the inhibitory crossed projections and might be involved in left–right alternation in the spinal cord of neonatal rodents (Hinckley et al., 2005).

Excitatory CINs are also active in binding left–right motor synergies along the length of the lumbar cord during locomotion in rodents (Butt and Kiehn, 2003). Whether glutamatergic CINs play a similar role in the lamprey (Biro et al., 2008) or other vertebrate species is unknown (Roberts, 2000; Grillner, 2003; Kiehn, 2006; Jankowska, 2008). However, populations of glutamatergic CINs found in both fish and mammals seem to be directly involved in coordinating the left–right synchronous activity observed after blocking all glycinergic and/or GABAergic synaptic transmission in the cord (Roberts, 2000; Grillner, 2003; Kiehn, 2006; Jankowska, 2008).

In addition to coordinating left–right activities in the CPG, CINs seem to play a role in setting the speed of locomotion. Thus, selective activation of the locomotor network on one side of the cord (Kjaerullf and Kiehn, 1997) or in the surgically isolated hemicord (Bonnot et al., 2002) in rodents always leads to a slower rhythm than observed in the intact cord. A change in the speed of fictive locomotion has also been reported after hemisection in the lamprey (Cangiano and Grillner, 2003). Here, the changes in swimming frequencies depend on the initial pharmacology or stimulation used to evoke swimming before the hemisection. In the zebrafish, ablation of a type of glutamatergic CINs—the ventrally located multipolar commissural descending interneurons—has been shown to affect slow frequency movements but not fast movements (McLean et al., 2007). Genetic ablation experiments in the mouse spinal cord have also ascribed to ventrally located putative excitatory CINs a role in stabilizing the rhythmic motor output (Zhang et al., 2008). Together, these experiments suggest a direct role of CINs in rhythm generation in addition to a role in left–right coordination.

CONCLUSION

The present study shows that CIN projections in the area of the upper lumbar spinal cord of the neonatal rodent that contains locomotor CPG circuits are heterogeneous, with at least four different putative neurotransmitter phenotypes. The relative proportions of putative excitatory and inhibitory projections suggest that both glycinergic and GABAergic CIN systems may play major roles in coordinating left–right motor activity in neonatal rodents. The low incidence of coexpression of putative glycinergic and GABAergic phenotypes sug-

gests that these inhibitory CIN transmitter pathways may be controlled independently. Finally, we did not observe any topographic segregation of the four CIN phenotypes. Understanding the anatomical organization of the CIN pathways will facilitate the comparison of different CIN populations among vertebrate species and among transgenic mouse models in which different patterns of locomotion may result from specific changes in the balance of crossed excitation and inhibition.

ACKNOWLEDGMENTS

We thank Mette Kirkegaard for comments on a previous version of the article, and Lovisa Källman and Anna Eriksson for caretaking and breeding of the different transgenic lines used in this study.

LITERATURE CITED

Allain AE, Bairi A, Meyrand P, Branchereau P. 2006. Expression of the glycinergic system during the course of embryonic development in the mouse spinal cord and its co-localization with GABA immunoreactivity. J Comp Neurol 496:832–846.

Alvarez FJ, Jonas PC, Sapir T, Hartley R, Berrocal MC, Geiman EJ, Todd AJ, Goulding M. 2005. Postnatal phenotype and localization of spinal cord V1 derived interneurons. J Comp Neurol 493:177–192.

Bannatyne BA, Edgley SA, Hammar I, Jankowska E, Maxwell DJ. 2003. Networks of inhibitory and excitatory commissural interneurons mediating crossed reticulospinal actions. Eur J Neurosci 18:2273–2284.

Bink K, Walch A, Feuchtinger A, Eisenmann H, Hutzler P, Hofler H, Werner M. 2001. TO-PRO-3 is an optimal fluorescent dye for nuclear counterstaining in dual-colour FISH on paraffin sections. Histochem Cell Biol 115:293–299.

Birinyi A, Viszokay K, Wéber I, Kiehn O, Antal M. 2003. Synaptic targets of commissural interneurons in the lumbar spinal cord of neonatal rats. J Comp Neurol 461:429–440.

Biro Z, Hill RH, Grillner S. 2008. The activity of spinal commissural interneurons during fictive locomotion in the lamprey. J Neurophysiol 100: 716–722.

Bonnot A, Morin D, Viala D. 1998. Organization of rhythmic motor patterns in the lumbosacral spinal cord of neonate mouse. Ann N Y Acad Sci 860:432–435.

Bonnot A, Whelan PJ, Mentis GZ, O'Donovan MJ. 2002. Locomotor-like activity generated by the neonatal mouse spinal cord. Brain Res Brain Res Rev 40:141–151.

Bracci E, Ballerini L, Nistri A. 1996. Localization of rhythmogenic networks responsible for spontaneous bursts induced by strychnine and bicuculline in the rat isolated spinal cord. J Neurosci 16:7063–7076.

Buchanan JT. 1982. Identification of interneurons with contralateral, caudal axons in the lamprey spinal cord: synaptic interactions and morphology. J Neurophysiol 47:961–975.

Buchanan JT. 1999. The roles of spinal interneurons and motoneurons in the lamprey locomotor network. Prog Brain Res 123:311–321.

Buchanan JT, Cohen AH. 1982. Activities of identified interneurons, motoneurons, and muscle fibers during fictive swimming in the lamprey and effects of reticulospinal and dorsal cell stimulation. J Neurophysiol 47:948–960.

Buchanan JT, Grillner S. 1987. Newly identified 'glutamate interneurons' and their role in locomotion in the lamprey spinal cord. Science 236: 312–314.

Butt SJ, Kiehn O. 2003. Functional identification of interneurons responsible for left-right coordination of hindlimbs in mammals. Neuron 38: 953–963.

Cangiano L, Grillner S. 2003. Fast and slow locomotor burst generation in the hemispinal cord of the lamprey. J Neurophysiol 89:2931–2942.

Cazalets JR, Borde M, Clarac F. 1996. The synaptic drive from the spinal locomotor network to motoneurons in the newborn rat. J Neurosci 16:298–306.

Christie KJ, Whelan PJ. 2005. Monoaminergic establishment of rostrocaudal gradients of rhythmicity in the neonatal mouse spinal cord. J Neurophysiol 94:1554–1564.

Clarke JD, Roberts A. 1984. Interneurones in the Xenopus embryo spinal cord: sensory excitation and activity during swimming. J Physiol 354: 345–362.

Cowley KC, Schmidt BJ. 1997. Regional distribution of the locomotor pattern-generating network in the neonatal rat spinal cord. J Neurophysiol 77:247–259.

Crone SA, Quinlan KA, Zagoraiou L, Droho S, Restrepo CE, Lundfald L, Endo T, Setlak J, Jessell TM, Kiehn O, Sharma K. 2008. Genetic ablation of V2a ipsilateral interneurons disrupts left-right locomotor coordination in mammalian spinal cord. Neuron 60:70–83.

Dale N. 1985. Reciprocal inhibitory interneurones in the Xenopus embryo spinal cord. J Physiol 363:61–70.

Dale N, Ottersen OP, Roberts A, Storm-Mathisen J. 1986. Inhibitory neurones of a motor pattern generator in Xenopus revealed by antibodies to glycine. Nature 324:255–257.

Eide AL, Glover J, Kjaerulff O, Kiehn O. 1999. Characterization of commissural interneurons in the lumbar region of the neonatal rat spinal cord. J Comp Neurol 403:332–345.

Feldblum S, Dumoulin A, Anoal M, Sandillon F, Privat A. 1995. Comparative distribution of GAD65 and GAD67 mRNAs and proteins in the rat spinal cord supports a differential regulation of these two glutamate decarboxylases in vivo. J Neurosci Res 42:742–757.

Fetcho JR. 1990. Morphological variability, segmental relationships, and functional role of a class of commissural interneurons in the spinal cord of goldfish. J Comp Neurol 299:283–298.

Gabbay H, Delvolve I, Lev-Tov A. 2002. Pattern generation in caudal-lumbar and sacrococcygeal segments of the neonatal rat spinal cord. J Neurophysiol 88:732–739.

Glover J. 1995. Retrograde and anterograde axonal tracing with fluorescent dextrans in the embryonic nervous system. Neurosci Protoc 30: 1–13.

Grillner S. 2003. The motor infrastructure: from ion channels to neuronal networks. Nat Rev Neurosci 4:573–586.

Herzog E, Landry M, Buhler E, Bouali-Benazzouz R, Legay C, Henderson CE, Nagy F, Dreyfus P, Giros B, El Mestikawy S. 2004. Expression of vesicular glutamate transporters, VGLUT1 and VGLUT2, in cholinergic spinal motoneurons. Eur J Neurosci 20:1752–1760.

Higashijima S, Mandel G, Fetcho JR. 2004a. Distribution of prospective glutamatergic, glycinergic, and GABAergic neurons in embryonic and larval zebrafish. J Comp Neurol 480:1–18.

Higashijima S, Schaefer M, Fetcho JR. 2004b. Neurotransmitter properties of spinal interneurons in embryonic and larval zebrafish. J Comp Neurol 480:19–37.

Hinckley C, Seebach B, Ziskind-Conhaim L. 2005. Distinct roles of glycinergic and GABAergic inhibition in coordinating locomotor-like rhythms in the neonatal mouse spinal cord. Neuroscience 131:745–758.

Huang J, Wang, Y, Wang W, Li Y, Wu S. 2008a. Proenkephalin mRNA is expressed in a subpopulation of GABAergic neurons in the spinal dorsal horn of the GAD67-GFP knock in mouse. Anat Record 291: 1334–1341.

Huang J, Wang Y, Wang W, Li Y, Tamamaki N, Wu S. 2008b. 5-HT3a receptor subunit is expressed in a subpopulation of GABAergic and enkephalinergic neurons in the mouse spinal cord. Neurosci Lett 441: 1–6.

Hughes DI, Mackie M, Nagy GG, Riddell JS, Maxwell DJ, Szabo G, Erdelyi F, Veress G, Szucs P, Antal M, Todd AJ. 2005. P boutons in lamina IX of the rodent spinal cord express high levels of glutamic acid decarboxylase-65 and originate from cells in deep medial dorsal horn. Proc Natl Acad Sci U S A 102:9038–9043.

Jankowska E. 2008. Spinal interneuronal networks in the cat: elementary components. Brain Res Rev 57:46–55.

Jankowska E, Hammar I, Slawinska U, Maleszak K, Edgley SA. 2003. Neuronal basis of crossed actions from the reticular formation on feline hindlimb motoneurons. J Neurosci 23:1867–1878.

Jankowska E, Edgley SA, Krutki P, Hammar I. 2005a. Functional differentiation and organization of feline midlumbar commissural interneurones. J Physiol 565(Pt 2):645–658.

Jankowska E, Krutki P, Matsuyama K. 2005b. Relative contribution of Ia inhibitory interneurones to inhibition of feline contralateral motoneurones evoked via commissural interneurones. J Physiol 568(Pt 2):617–628.

Jankowska E, Stecina K, Cabaj A, Pettersson LG, Edgley SA. 2006. Neuronal relays in double crossed pathways between feline motor cortex and ipsilateral hindlimb motoneurones. J Physiol 575(Pt 2):527–541.

Jankowska E, Bannatyne BA, Stecina K, Hammar I, Cabaj A, Maxwell DJ. 2009. Commissural interneurons with input from group I and II muscle afferents in feline lumbar segments: neurotransmitters, projections and target cells. J Physiol 587:401–418.

Jonas P, Bischofberger J, Sandkuhler J. 1998. Corelease of two fast neurotransmitters at a central synapse. Science 281:419–424.

Kiehn O. 2006. Locomotor circuits in the mammalian spinal cord. Annu Rev Neurosci 29:279–306.

Kiehn O, Kjaerulff O. 1998. Distribution of central pattern generators for rhythmic motor outputs in the spinal cord of limbed vertebrates. Ann N Y Acad Sci 860:110–129.

Kiehn O, Quinlan KA, Restrepo CE, Lundfald L, Borgius L, Talpalar AE, Endo T. 2008. Excitatory components of the mammalian locomotor CPG. Brain Res Rev 57:56–63.

Kjaerulff O, Kiehn O. 1996. Distribution of networks generating and coordinating locomotor activity in the neonatal rat spinal cord in vitro: a lesion study. J Neurosci 16:5777–5794.

Kremer E, Lev-Tov A. 1997. Localization of the spinal network associated with generation of hindlimb locomotion in the neonatal rat and organization of its transverse coupling system. J Neurophysiol 77:1155–1170.

Kudo N, Yamada T. 1987. N-methyl-D,L-aspartate-induced locomotor activity in a spinal cord-hindlimb muscles preparation of the newborn rat studied in vitro. Neurosci Lett 75:43–48.

Kullander K, Butt SJ, Lebret JM, Lundfald L, Restrepo CE, Rydstrom A, Klein R, Kiehn O. 2003. Role of EphA4 and EphrinB3 in local neuronal circuits that control walking. Science 299:1889–1892.

Lopez-Bendito G, Sturgess K, Erdelyi F, Szabo G, Molnar Z, Paulsen O. 2004. Preferential origin and layer destination of GAD65-GFP cortical interneurons. Cereb Cortex 14:1122–1133.

Lundfald L, Restrepo CE, Butt SJ, Peng CY, Droho S, Endo T, Zeilhofer HU, Sharma K, Kiehn O. 2007. Phenotype of V2-derived interneurons and their relationship to the axon guidance molecule EphA4 in the developing mouse spinal cord. Eur J Neurosci 26:2989–3002.

Ma W, Behar T, Chang L, Barker JL. 1994. Transient increase in expression of GAD65 and GAD67 mRNAs during postnatal development of rat spinal cord. J Comp Neurol 346:151–160.

Mackie M, Hughes DI, Maxwell DJ, Tillakaratne NJ, Todd AJ. 2003. Distribution and colocalisation of glutamate decarboxylase isoforms in the rat spinal cord. Neuroscience 119:461–472.

Matsuura J, Ajiki K, Ichikawa T, Misawa H. 1997. Changes of expression levels of choline acetyltransferase and vesicular acetylcholine transporter mRNAs after transection of the hypoglossal nerve in adult rats. Neurosci Lett 236:95–98.

Matsuyama K, Nakajima K, Mori F, Aoki M, Mori S. 2004. Lumbar commissural interneurons with reticulospinal inputs in the cat: morphology and discharge patterns during fictive locomotion. J Comp Neurol 474: 546–561.

Matsuyama K, Kobayashi S, Aoki M. 2006. Projection patterns of lamina VIII commissural neurons in the lumbar spinal cord of the adult cat: an anterograde neural tracing study. Neuroscience 140:203–218.

McLean DL, Fan J, Higashijima S, Hale ME, Fetcho JR. 2007. A topographic map of recruitment in spinal cord. Nature 446:71–75.

Mentel T, Krause A, Pabst M, El Manira A, Buschges A. 2006. Activity of fin muscles and fin motoneurons during swimming motor pattern in the lamprey. Eur J Neurosci 23:2012–2026.

Mentis GZ, Alvarez FJ, Bonnot A, Richards DS, Gonzalez-Forero D, Zerda R, O'Donovan MJ. 2005. Noncholinergic excitatory actions of motoneurons in the neonatal mammalian spinal cord. Proc Natl Acad Sci U S A 102:7344–7349.

Nakayama K, Nishimaru H, Kudo N. 2002. Basis of changes in left-right coordination of rhythmic motor activity during development in the rat spinal cord. J Neurosci 22:10388–10398.

Nishimaru H, Restrepo CE, Ryge J, Yanagawa Y, Kiehn O. 2005. Mammalian motor neurons corelease glutamate and acetylcholine at central synapses. Proc Natl Acad Sci U S A 102:5245–5249.

Nishimaru H, Restrepo CE, Kiehn O. 2006. Activity of Renshaw cells during locomotor-like rhythmic activity in the isolated spinal cord of neonatal mice. J Neurosci 26:5320–5328.

Nissen UV, Mochida H, Glover JC. 2005. Development of projection-specific interneurons and projection neurons in the embryonic mouse and rat spinal cord. J Comp Neurol 483:30–47.

Oliveira AL, Hydling F, Olsson E, Shi T, Edwards RH, Fujiyama F, Kaneko T, Hokfelt T, Cullheim S, Meister B. 2003. Cellular localization of three vesicular glutamate transporter mRNAs and proteins in rat spinal cord and dorsal root ganglia. Synapse 50:117–129.

Pow DV, Wright LL, Vaney DI. The immunocytochemical detection of amino-acid neurotransmitters in paraformaldehyde-fixed tissues. 1995. J Neurosci Methods 56:115–123.

Poyatos I, Ponce J, Aragon C, Gimenez C, Zafra F. 1997. The glycine transporter GLYT2 is a reliable marker for glycine-immunoreactive neurons. Brain Res Mol Brain Res 49:63–70.

Quinlan KA, Kiehn O. 2007. Segmental, synaptic actions of commissural interneurons in the mouse spinal cord. J Neurosci 27:6521–6530.

Rende M, Giambanco I, Buratta M, Tonali P. 1995. Axotomy induces a different modulation of both low-affinity nerve growth factor receptor and choline acetyltransferase between adult rat spinal and brainstem motoneurons. J Comp Neurol 363:249–263.

Roberts A. 2000. Early functional organization of spinal neurons in developing lower vertebrates. Brain Res Bull 53:585–593.

Ryge J, Westerdahl AC, Alstrøm P, Kiehn O. 2008. Gene expression profiling of two distinct neuronal populations in the rodent spinal cord. PLoS ONE. 3:e3415.

Soffe SR, Zhao FY, Roberts A. 2001. Functional projection distances of spinal interneurons mediating reciprocal inhibition during swimming in Xenopus tadpoles. Eur J Neurosci 13:617–627.

Stokke MF, Nissen UV, Glover JC, Kiehn O. 2002. Projection patterns of commissural interneurons in the lumbar spinal cord of the neonatal rat. J Comp Neurol 446:349–359.

Storm-Mathisen J, Leknes AK, Bore AT, Vaaland JL, Edminson P, Haug FM, Ottersen OP. 1983. First visualization of glutamate and GABA in neurones by immunocytochemistry. Nature 301:517–520.

Stornetta RL, McQuiston TJ, Guyenet PG. 2004. GABAergic and glycinergic presympathetic neurons of rat medulla oblongata identified by retrograde transport of pseudorabies virus and in situ hybridization. J Comp Neurol 479:257–270.

Tamamaki N, Yanagawa Y, Tomioka R, Miyazaki J, Obata K, Kaneko T. 2003. Green fluorescent protein expression and colocalization with calretinin, parvalbumin, and somatostatin in the GAD67-GFP knock-in mouse. J Comp Neurol 467:60–79.

Weber I, Veress G, Szucs P, Antal M, Birinyi A. 2007. Neurotransmitter systems of commissural interneurons in the lumbar spinal cord of neonatal rats. Brain Res 1178:65–72.

Wilson NR, Kang J, Hueske EV, Leung T, Varoqui H, Murnick JG, Erickson JD, Liu G. 2005. Presynaptic regulation of quantal size by the vesicular glutamate transporter VGLUT1. J Neurosci 25:6221–6234.

Wojcik SM, Katsurabayashi S, Guillemin I, Friauf E, Rosenmund C, Brose N, Rhee JS. 2006. A shared vesicular carrier allows synaptic corelease of GABA and glycine. Neuron 50:575–587.

Zafra F, Aragon C, Gimenez C. 1997. Molecular biology of glycinergic neurotransmission. Mol Neurobiol 14:117–142.

Zeilhofer HU, Studler B, Arabadzisz D, Schweizer C, Ahmadi S, Layh B, Bosl MR, Fritschy JM. 2005. Glycinergic neurons expressing enhanced green fluorescent protein in bacterial artificial chromosome transgenic mice. J Comp Neurol 482:123–141.

Zhang Y, Narayan S, Geiman E, Lanuza GM, Velasquez T, Shanks B, Akay T, Dyck J, Pearson K, Gosgnach S, Fan CM, Goulding M. 2008. V3 spinal neurons establish a robust and balanced locomotor rhythm during walking. Neuron 60:84–96.

Zhong G, Díaz-Ríos M, Harris-Warrick RM. 2006. Intrinsic and functional differences among commissural interneurons during fictive locomotion and serotonergic modulation in the neonatal mouse. J Neurosci 26: 6509–6517.